Liquid Crystals
Publication details, including instructions for authors and subscription information:
http://www.tandfonline.com/loi/tlct20

Effect of an electric field on defects in a nematic liquid crystal with variable surface anchoring

T. Arun Kumar [a], V.S.S. Sastry [a], Ken Ishikawa [b], Hideo Takezoe [b], N.V. Madhusudana [c] & Surajit Dhara [a]

[a] School of Physics, University of Hyderabad, Hyderabad, 500046, India

[b] Department of Organic and Polymeric Materials,, Tokyo Institute of Technology, 2-12-1-S8-42 O-okayama, Meguro-ku, Tokyo, 152-8552, Japan

[c] Raman Research Institute, C.V. Raman Avenue, Bangalore, 560080, India

Available online: 12 Aug 2011

To cite this article: T. Arun Kumar, V.S.S. Sastry, Ken Ishikawa, Hideo Takezoe, N.V. Madhusudana & Surajit Dhara (2011): Effect of an electric field on defects in a nematic liquid crystal with variable surface anchoring, Liquid Crystals, 38:8, 971-979

To link to this article: http://dx.doi.org/10.1080/02678292.2011.587962

Liquid Crystals,
Vol. 38, No. 8, August 2011, 971–979

Taylor & Francis
Taylor & Francis Group

Effect of an electric field on defects in a nematic liquid crystal with variable surface anchoring

T. Arun Kumar[a], V.S.S. Sastry[a], Ken Ishikawa[b], Hideo Takezoe[b], N.V. Madhusudana[c] and Surajit Dhara[a]*

[a]*School of Physics, University of Hyderabad, Hyderabad-500046, India;* [b]*Department of Organic and Polymeric Materials, Tokyo Institute of Technology, 2-12-1-S8-42 O-okayama, Meguro-ku, Tokyo-152-8552, Japan;* [c]*Raman Research Institute, C.V. Raman Avenue, Bangalore-560080, India*

(*Received 22 January 2011; final version received 10 May 2011*)

We report experimental studies on defects in a nematic liquid crystal with negative dielectric anisotropy mounted in a cell with perfluoropolymer-coated surfaces. The sample exhibits a discontinuous anchoring transition from planar to homeotropic on cooling at zero or a small electric field, and above a cross-over voltage a continuous 'inverse Freedericksz transition', at which the director starts tilting in opposite directions at the two surfaces. Defects of strength $\pm 1/2$ are either annihilated or expelled when the director tilts. On the other hand, disclination lines of ± 1 which end in partial point defects (boojums) at the surfaces in the planar alignment regime acquire point defects of strength ± 1 at the midplane of the cell when the director tilts. At a low enough temperature, the homeotropic anchoring becomes strong, and an electric field above the Freedericksz threshold generates the usual umbilic defects, which follow the dynamic scaling laws found in earlier studies.

Keywords: defects; surface anchoring; annihilation; boojums

1. Introduction

Liquid crystals exhibit a variety of colourful textures under a polarising optical microscope [1]. These textures are useful for the preliminary characterisation of the liquid crystalline phases. For example, nematic liquid crystals generally exhibit schlieren textures. Cholesteric and smectic liquid crystals exhibit fingerprint and focal conic textures. These textures are composed of different types of defects [2, 3]. In nematics the characteristic defects are disclinations which are basically line defects. In smectics, in addition to the focal conic defects, dislocations exist as line defects, although they cannot be seen optically. The line defects are topological defects in order parameter space. They are also seen in various other systems: for example, vortices in superfluid helium, dislocations in crystals [4]. The disclinations seen in nematics have been studied extensively, both theoretically and experimentally [5–15]. Two disclinations attract each other when they are 'unlike' and repel when they are 'like', mimicking the interactions between electrical charges. In a classic paper Nehring and Saupe [6] presented detailed observations on schlieren textures of nematics and calculated the force of interaction between two disclinations. They showed that annihilation of unlike half-strength defects and creation of integer-strength defects from merger of like half-strength defects sometimes occur very near the nematic–isotropic phase transition temperature. Lavrentovich *et al.* [16] have studied both theoretically and experimentally different types of defects and their structures in various liquid crystals.

There are also several experimental and theoretical studies on the defect–antidefect annihilation dynamics in nematic liquid crystals [17–20]. The annihilation dynamics have been studied as functions of time, when the director field evolves after rapid quenching from isotropic to nematic phase. Bogi *et al.* have studied the influence of surface anchoring on the annihilation dynamics of two parallel $\pm 1/2$ defects. They found that when the defect lines are far from each other, the elastic interaction is completely screened by anchoring energy [17]. The dynamics of $\pm 1/2$ defects under an external electric field was investigated by Blanc *et al.* [18]. They found that the relaxation is governed by the π wall connecting two opposite charges and that the $+1/2$ defects move faster than $-1/2$ defects.

Recently we reported the observation of a strong discontinuous anchoring transition at ~47.5°C from planar to homeotropic on cooling, and the reverse transition at ~50.6°C on heating in a nematic liquid crystal (CCN-47) on perfluoropolymer-coated surfaces [21, 22]. In the cooling mode, the sample exhibits a texture with a large number of $\pm 1/2$ defects above ~47.5°C, and we have reported earlier

*Corresponding author. Email: sdsp@uohyd.ernet.in

ISSN 0267-8292 print/ISSN 1366-5855 online

DOI: 10.1080/02678292.2011.587962
http://www.informaworld.com

about the defect–antidefect correlations in this system [23]. There are several experimental investigations reported on CCN-47 [24–30]. Very recently, using the same compound, we have fabricated a bistable device by exploiting the large hysteresis region of the discontinuous anchoring transition [24, 25] in a rubbed cell. In this paper we report observations on the merging of two like half-strength defects to form integer strength (± 1) defects and annihilation of two unlike half-strength defects when the director tilts away from planar alignment. The tilting occurs below the anchoring transition temperature under applied electric fields which are large enough to change the transition to a continuous one. We argue that the defects of strength 1 which are seen just below this temperature have a new structure, with either a + or a − point defect located at the midplane of the sample, and associated with two boojums lying at the two surfaces. Their number density decreases as the temperature is reduced. At a temperature $\sim 6°$ below the anchoring transition temperature, the anchoring strength for homeotropic alignment grows to a large value, and sample leads to the formation of umbilics. We find that these field-induced defects follow the dynamic scaling laws found earlier for both umbilics and schlieren defects near the NI transition temperature.

2. Experimental details

We used a perfluoropolymer, namely, poly[perfluoro (4-vinyloxy-1-butene)] known as CYTOP (Asahi Glass Co., Ltd) deposited on indium tin oxide (ITO)-coated glass plates as the alignment layer. CYTOP is commonly used as an antireflection coating for organic light-emitting devices. We have reported recently that it can be used as a perfect homeotropic alignment layer for the smectic liquid crystals [26]. In the present experiment we spin coated CYTOP on ITO-coated glass plates which were used to construct experimental cells. Typical thickness of the cells used in the experiments was ~ 5.2 μm. The nematic liquid crystal, 4′-butyl-4-heptyl-bicyclohexyl-4-carbonitrile (CCN-47) was filled in the cell in the isotropic phase by capillary action. The chemical structures of CCN-47 and CYTOP are shown in Figure 1(a). The liquid crystal compound exhibits the following phase transitions: Cr 25.6°C Sm–A 28.2°C N 57.3°C I and a large negative dielectric anisotropy ($\Delta\epsilon = -5.7$ at 30°C). Texture observations were made by using a polarising optical microscope (Olympus BX-51). The temperature of the sample was controlled by mounting it in a Mettler hotstage. A signal generator was used to apply voltages at a frequency of 3.11 kHz.

3. Results and discussion

3.1 Textures without an electric field

We first show the textures observed under a polarising microscope in the absence of an electric field. The compound exhibits a planar texture just below the nematic–isotropic phase transition temperature (57.3°C). A typical planar texture at 52.2°C with mostly half-strength disclinations is shown in Figure 1(b). The discontinuous anchoring transition, the details of which have been described earlier [21], starts at $\sim 47.5°$C (Figure 1(c)) in a few locations, and the sample becomes completely homeotropic as it is cooled down (Figure 1(d)). The system also exhibits a large hysteresis of a few degrees Celsius in the anchoring transition temperature.

We observed textures as the sample was heated at a rate of 1° per minute from the homeotropic state (Figure 2(a)). During heating the sample starts to undergo the discontinuous anchoring transition at 50.6°C from homeotropic to planar (Figure 2(b)). Only integer strength defects with many walls associated with homeotropic to planar transitions are seen (Figure 2(c)). As the director reorients from homeotropic to planar via tilted orientation, only integer strength defects can be expected to form in the sample. The defect density is much lower compared with that of the field-induced umbilic defects which are discussed later. On further heating the dark brushes become comparatively thicker (Figure 2(d)). In several heating cycles defects are found to appear at the same locations showing that the director distortion starts at the glass plates.

On cooling the sample under the action of an AC electric field, the anchoring transition temperature is found to decrease with the field. The details of the theoretical and experimental results have been reported elsewhere [22]. The transition continues to be a discontinuous one from planar to homeotropic up to a cross-over voltage of ~ 0.5 V. Above this voltage, the anchoring transition becomes continuous, the tilt angles at the two surfaces just start to deviate from zero at the transition point, and increase in magnitude as the temperature is lowered further. Our experimental results could only be explained by assuming that the tilt angles at the two surfaces have *opposite* signs, so that the director retains an orientation parallel to the glass plates at the midplane of the sample. Thus, the above transition could be

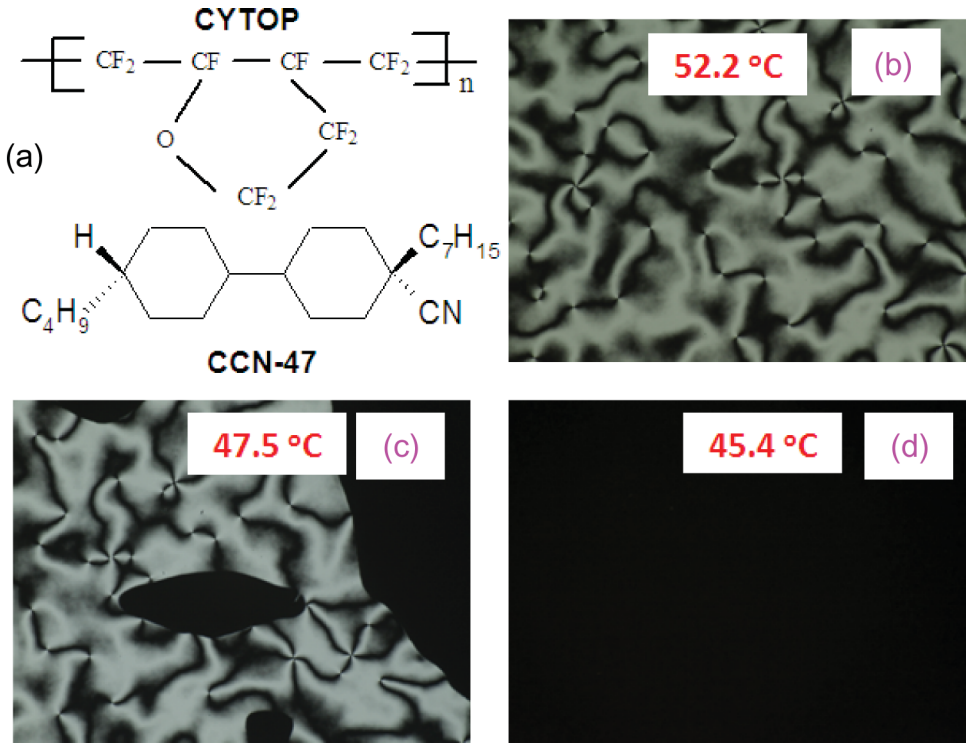

Figure 1. (a) Chemical structures of the perfluoropolymer alignment layer (CYTOP) and the liquid crystal (CCN-47); (b) photomicrographs of the texture at 52.2°C; (c) during discontinuous anchoring transition at 47.5°C; (d) homeotropic texture at 45.4°C. The observation was made in the absence of an electric field using a 5.2 μm cell (colour version online).

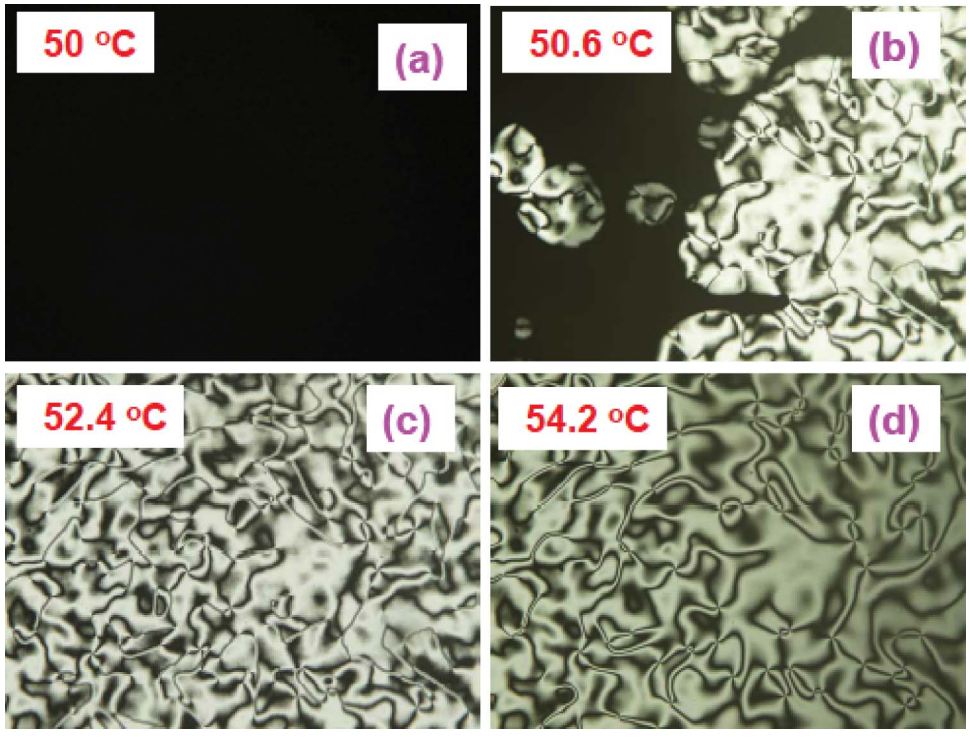

Figure 2. Photomicrographs showing discontinuous anchoring transition on heating the sample from homeotropic state: (a) homeotropic texture at 50°C; (b) during the discontinuous anchoring transition at 50.6°C; (c) planar texture at 52.4°C; and (d) at 54.2°C. The observation was made in the absence of an electric field using a 5.2 μm cell (colour version online).

described as an 'inverse Freedericksz transition' [22]. As we shall see, the opposite tilts induced by the field at the two surfaces give rise to a new type of defect structure in the sample.

3.2 Textures with electric field

In Figure 3 we show the textures under the application of a sine wave voltage of 0.9 V at a frequency 3.11 kHz. No observable change in the texture is observed at temperatures above that corresponding to the anchoring transition (Figure 3(a)). This is expected as the dielectric anisotropy of the sample is negative and the field is perpendicular to the glass plates. When the temperature is reduced to the transition point, some domains with lower birefringence start growing in the sample. This is a signature of the continuous anchoring transition, at which the director starts tilting away from the two surfaces (Figure 3(b)). These domains again start from the same locations at which the discontinuous transition occurs at low voltages, showing that the CYTOP coating has some non-uniformity. Like half-strength defects merge together to form defects with integer strength (± 1) or are expelled from the tilted domains. Unlike half-disclinations annihilate each other (Figure 3(b) and (c)).

On cooling from the isotropic phase, the nematic director has planar alignment, as evidenced by the presence of half-strength disclination lines. We concentrate on disclinations of strength ± 1, which survive the continuous anchoring transition under the applied external electric field. The stability of the (non-topological) ± 1 disclinations arises because of the escape of the director in the third direction [7], removing the core of the line defect. Hereafter we call the ± 1 disclination line the line defect, although it contains no orientational singularity or core. However, they are lines connecting two point defects at the top and bottom surfaces (as described in the following). The director configurations of $+1$ and -1 line defects confined to a cell of finite thickness are shown in Figures 4 and 5, respectively. The top and side views of $+1$ defect are sketched in Figure 4. The director tilts away from the plane of the glass plates, the nail heads being at lower positions than the tips in Figure 4(a). The director configuration has rotational symmetry about the defect line (Figure 4(b)), and incorporates a partial '$+1$ point' disclination at the lower glass plate and a partial '-1 point' disclination at the upper surface. Such surface point defects are called boojums [31]. The top view of the -1 line defect is shown in Figure 5. Note that there is no rotational symmetry about the line

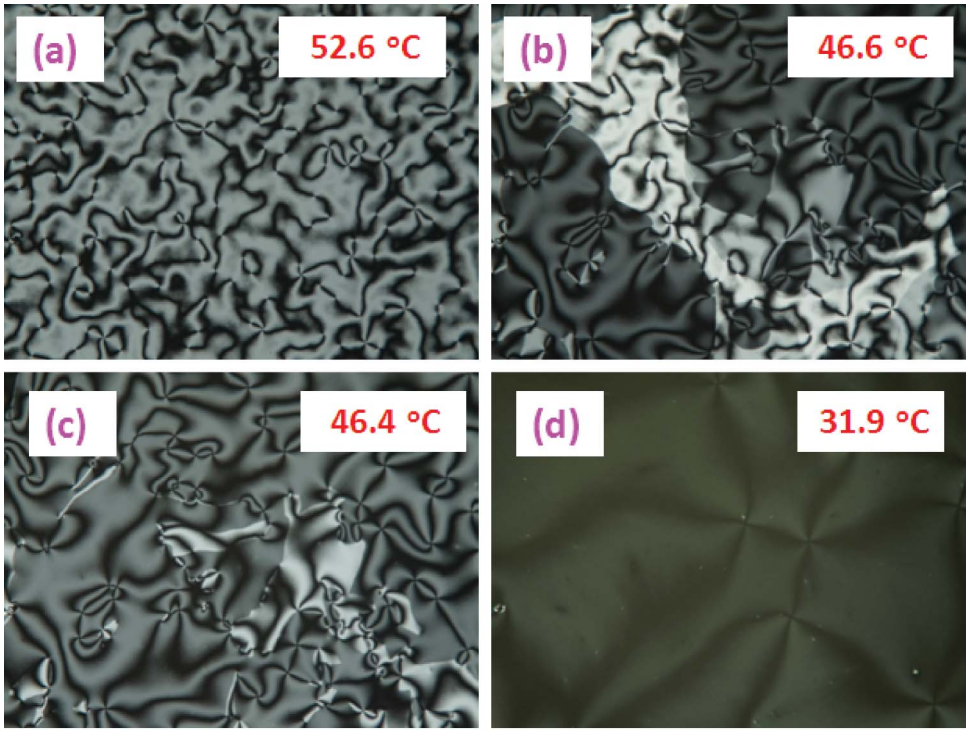

Figure 3. Photomicrographs showing anchoring transition under an applied AC voltage of 0.9 V and frequency of 3.11 kHz during cooling: (a) at 52.6°C; (b) showing a continuous anchoring transition at 46.6°C; (c) at 46.4°C; (d) dark field of view with a few four brush defects at 31.9°C. Cell thickness 5.2 μm (colour version online).

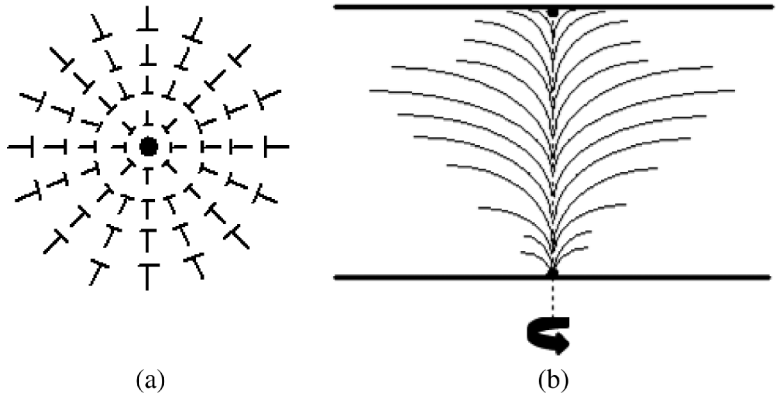

Figure 4. Schematic of director orientations of a +1 defect line: (a) top view; (b) side view.

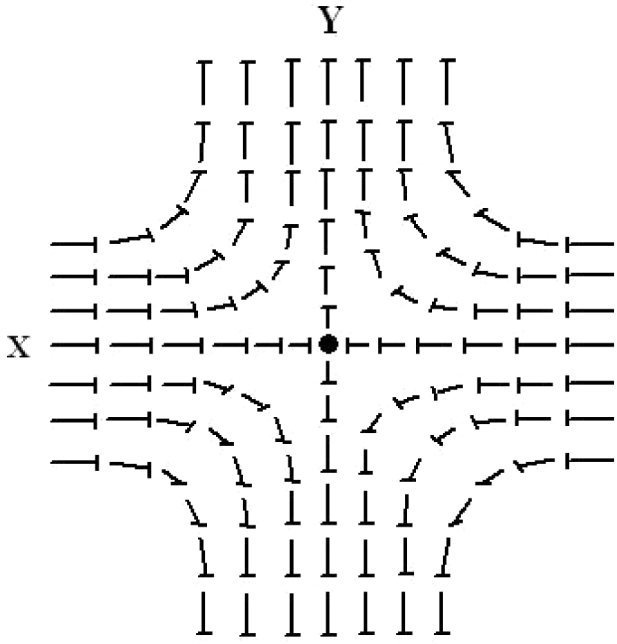

Figure 5. Schematic of director orientations in the top view of a −1 disclination line.

defect, along which there is a two-fold axis. As we move along the 45° line from lower right to upper left quadrant, the director twists in an anti-clockwise fashion. Looking along the lower left to upper right quadrant, the twist is clockwise. On the other hand, along the vertical and horizontal planes, there is only splay–bend distortion. Again near the upper and lower glass plates, there will be partial point defects or boojums of opposite signs.

We now focus our attention on a small region of the sample and carefully observe the merging and annihilation processes. We noticed that at 44.1°C some of the half-strength defects had already merged to form defects of strength one (Figure 6). There are still some half-strength defects and in a few cases the inversion walls connecting them can be clearly seen (see the [green] arrows [in colour online]). As the temperature is lowered the positions of one-strength defects are almost fixed and the half-strength defects move closer (Figure 6(b) and (c)). The half strength defects of the same sign also move closer to reduce the energy of the inversion wall. Finally two like half-strength defects merge to create a defect of strength one (Figure 6(d)). In the present case it is a +1. Two unlike half-strength defects are annihilated as shown in Figure 6(d). We also note that in a given pair of annihilating defects, the +1/2 defects move faster towards the −1/2 defect (Figure 6(a) and (b)) as reported by Blanc *et al.* [18]. Finally no half-strength defects remain in the texture (Figure 6(d)). When the electric field is switched off at any temperature below that of the anchoring transition, immediately homeotropic domains are formed and the field of view becomes completely dark recovering the discontinuous anchoring transition.

If the homeotropic anchoring at the surfaces is strong, an electric field of the appropriate magnitude applied along the director of a nematic with negative dielectric anisotropy induces the usual Freedericksz transition. In this case, the director starts tilting at the *midplane* of the sample and in view of the degeneracy in azimuthal angles, line defects of integral strength which are somewhat similar to those described above form in the sample. The strong homeotropic anchoring at the surfaces ensures that no boojums form at the ends of the line defects, which are called *umbilic* defects [2]. We describe observations on umbilic defects at low temperatures in Section 3.3.

In our sample, the boundary condition changes from planar to homeotropic below the anchoring transition temperature, presumably because of the build up of smectic-A-like short-range order on the

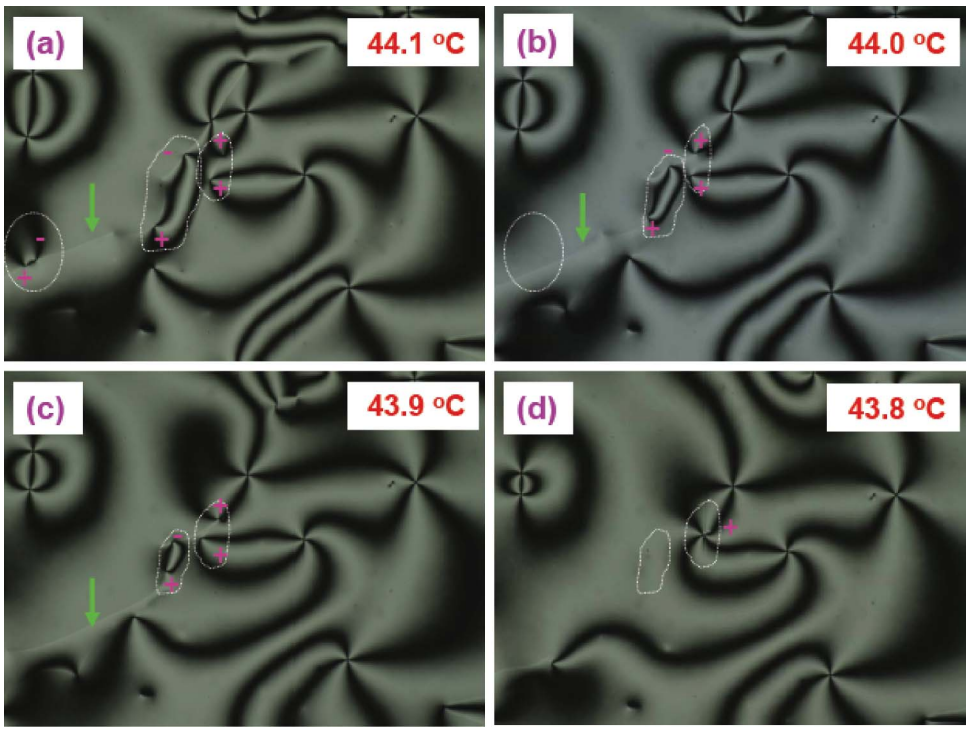

Figure 6. Merging of $\pm 1/2$ defects under the applied AC voltage of 1.5 V; (a) pairs of half-strength defects are shown with enclosed dotted white lines at 44.1°C; some of the half-strength defects have already merged to form integer-strength defects; (b) one pair of unlike defects (enclosed with dotted lines at the left) annihilated at 44°C; (c) both the unlike and like half-strength defects approach each other; (d) like half-strength defects merge to form an integer defect and unlike half-strength defects are annihilated. White wispy lines pointed by green arrows are inversion walls (colour version online).

flat surfaces of the cell walls as the temperature of the sample is lowered. As we have discussed earlier [22], this implies that the anchoring strength is weak close to the anchoring transition temperature. What will be the structures of the defects of strength 1 when the director tilts oppositely at the surfaces below the continuous anchoring transition temperature under the AC electric field?

In the case of a disclination line of strength +1, there are two possibilities consistent with the opposite tilts at the two surfaces: (i) the boojum with negative sign as in Figure 4(b) can detach from the surface and become a point disclination with strength −1 which settles down at the center of the sample, and a new boojum with positive sign is formed at the surface. Thus the disclination line now will have a collapse of the director occurring in opposite directions in the two halves of the cell (Figure 7(a)). (ii) Another possibility is for the positive boojum (of Figure 4(b)) to shift to the midplane as a +1 point defect, and a boojum of negative strength to form at the surface (Figure 7(b)). Both

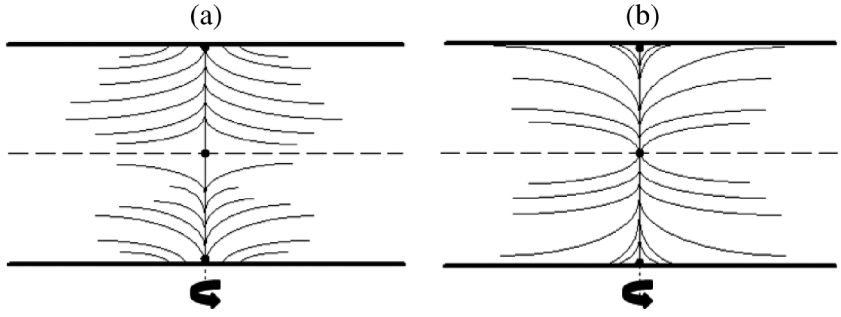

Figure 7. Schematic representation of two possible director configurations with opposite tilts at the two surfaces in the case of +1 defect.

of these field-induced structures have rotational symmetry about the line defects and exhibit similar dark brushes between crossed polarisers. As the temperature is lowered, the tilt angle increases near the surfaces and the overall brightness decreases.

The change in the director field in the presence of the external field can be expected to be more complicated in the case of a line defect of strength -1. The expected director patterns in the XZ and YZ planes which had only splay–bend distortions above the anchoring transition temperature are shown in Figure 8. Again there are only splay–bend distortions in these two planes, but it is clear that in any given quadrant, the twist distortion of the director changes sense between the upper and lower halves of the sample. The director structure here is more complicated than that of the point defect at the center of the sample shown in Figure 7(a) and (b). The projection of the director field in the XY-plane in one of the quadrants is shown to emphasise that the optical pattern between crossed polarisers will be similar to that of the line defect of -1 strength in the planar aligned sample. The overall pattern again has two-fold symmetry about the line defect as before. When the $+1$ and -1 line defects with these modified structures approach each other, it will be energetically less expensive if the $+1$ defect with structure as in Figure 7(a) approaches the -1 defect along the Y-axis, while that with the structure as in Figure 7(b) approaches along the X-axis. The opposite tilts of the director at the two plates below the continuous anchoring transition temperature in the presence of sufficiently high external electric field gives rise to the new type of structures illustrated above. Both line defects of $+1$ and -1 strength will have point defects at the midplane of the cell, apart from the two boojums at the two surfaces. The structures are new, which appear because of the opposite tilts at the two surfaces realised by the anchoring transition under an electric field: the field free line defects are not expected to have the point defects at the center. The umbilic defects seen above the Freedericksz threshold in materials with negative dielectric anisotropy in cells with strong homeotropic boundary conditions do not have the boojums. The interactions between the new types of defects in our sample can be expected to be dominated by the point defects at the midplane of the cells.

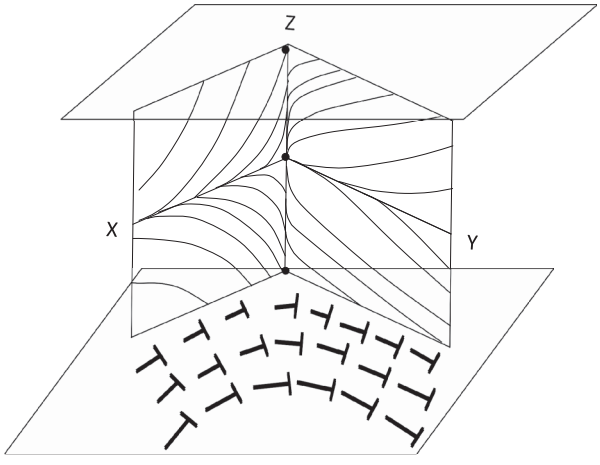

Figure 8. Some cross sections of the director configuration of -1 disclination, with opposite tilts at the two surfaces.

Although the structures of both $+1$ and -1 line defects change substantially below the inverse Freedericksz transition point, they continue to produce four dark brushes between crossed polarisers. On further cooling of the sample, the number of these defects is also reduced due to the mutual annihilation of defects of opposite strength, which can approach each other as described above. A typical texture on cooling the sample to 31.9°C which is much lower than the anchoring transition temperature is shown in Figure 3(d). The texture appears dark with a few four-brush defects remaining in the background.

3.3 Dynamics of umbilic defects

We further studied the dynamics of the field-induced umbilics that emerge from the homeotropic state when the anchoring energy is relatively strong. The details of annihilation dynamics of umbilic defects have been reported by Dierking *et al.* [20] in a commercially available mixture (ZLI-2806) on substrates treated with JALS-204-R40. In the present study the umbilic defects were induced by sine wave of amplitude 4 V and frequency of 3.11 kHz at the temperature of 42°C. As discussed in our earlier paper [22], the anchoring strength A is about 10^{-5} J m^{-2} at this temperature. Further, the bend elastic constant K_{33} is 0.8 pN (see [30]). Thus, the extrapolation length $K_{32}/A \simeq 0.08$ μm, which is much smaller than the sample thickness $d = 5.2$ μm. The anchoring energy is effectively *strong*, and the applied field induces umbilic defects above the Freedericksz threshold as discussed earlier. The recording and analysis of textures were carried out with the help of a suitable software.

Typical photographs showing the evolution of umbilic defects with time are shown in Figure 9. It is seen that initially there are a large number of ± 1 umbilic defects (Figure 9(a)), which mutually annihilate with the progress of time to reduce the number density (Figure 9(b)–(d)). Finally a small number remains static due to the surface irregularities or

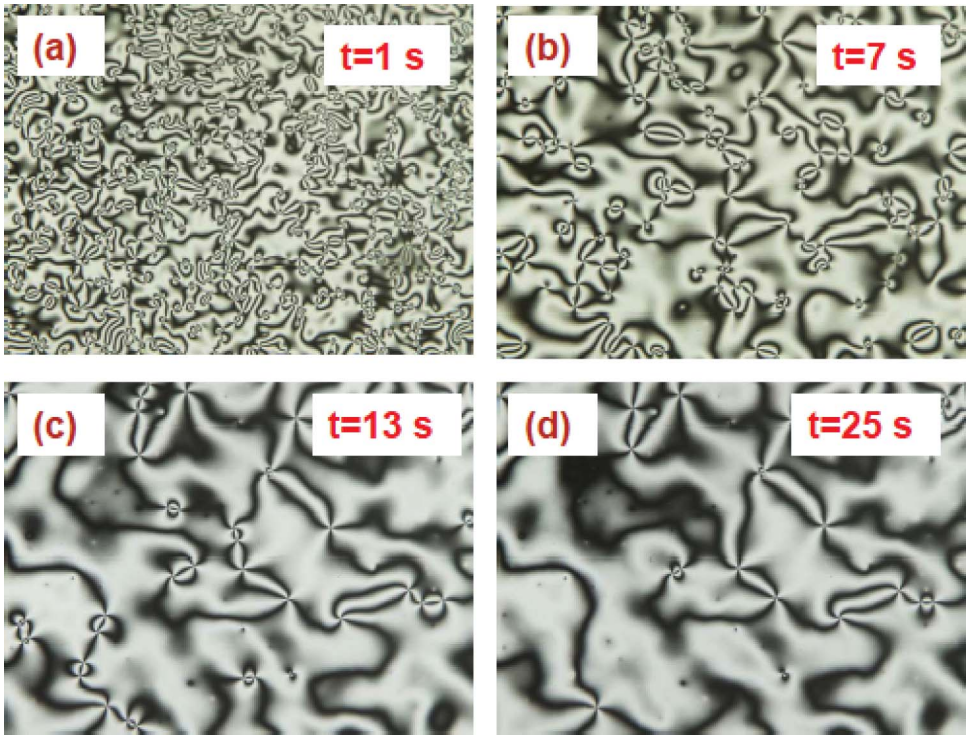

Figure 9. Textures (at 42°C) showing umbilic defects under an applied voltage of amplitude 4 V and frequency 3.11 kHz; elapsed time after the application of the field: (a) 1 s; (b) 7 s; (c) 13 s; and (d) 25 s. Cell thickness $d = 5.2$ μm (colour version online).

impurities (Figure 9(d)). The director field around a +1 strength umbilic defect is shown schematically in Figure 10. Diagrams showing the variations of defect density $\rho(t)$ and the inter-defect separation $D(t)$ as functions of time are shown in Figure 11(a) and (b), respectively. According to the theoretical predictions [12] the defect density and the inter-defect separation obey the following scaling laws:

$$\rho(t) \propto t^{-\nu} \tag{1}$$

with $\nu = 1$, and

$$D(t) \propto (t_0 - t)^{\alpha} \tag{2}$$

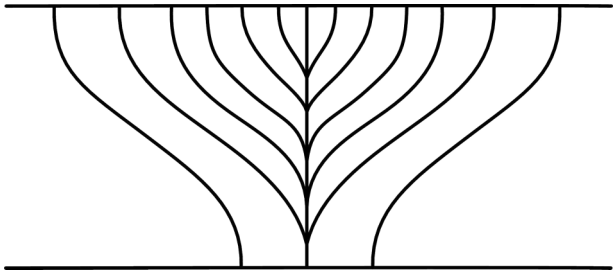

Figure 10. Schematic of director field of an umbilic defect of +1 strength generated by an electric field. Note the absence of boojums.

where $t_0 - t$ is the time to annihilate and $\alpha = 0.5$. A nonlinear least squares fitting program was used to fit the experimental data. The best fits to $\rho(t)$ and $D(t)$ are shown in Figure 11(a) and (b), respectively. The fit parameters are obtained as $\nu = 1.1 \pm 0.05$, and $\alpha = 0.55 \pm 0.01$, and are very close to the theoretical predictions. Similar values of the above two exponents have also been reported by Dierking *et al.* [20]. This study verifies previously reported results and suggests that irrespective of the material and alignment layers these critical exponents for umbilic defects are universal.

4. Conclusions

In conclusion, we have reported the evolution of line defects of strength 1 in a planar aligned sample to new types of defects, consisting of point defects of integral strength at the midplane, and boojums at the surfaces, as the sample is cooled below a continuous anchoring transition temperature under an electric field. We have recorded the annihilation of half-strength defects of opposite sign and creation of integer-strength defects from those of the same sign. We have also studied the dynamics of the umbilic defects formed under the action of an electric field on the homeotropically aligned state at a sufficiently low temperature, and found that the exponents for

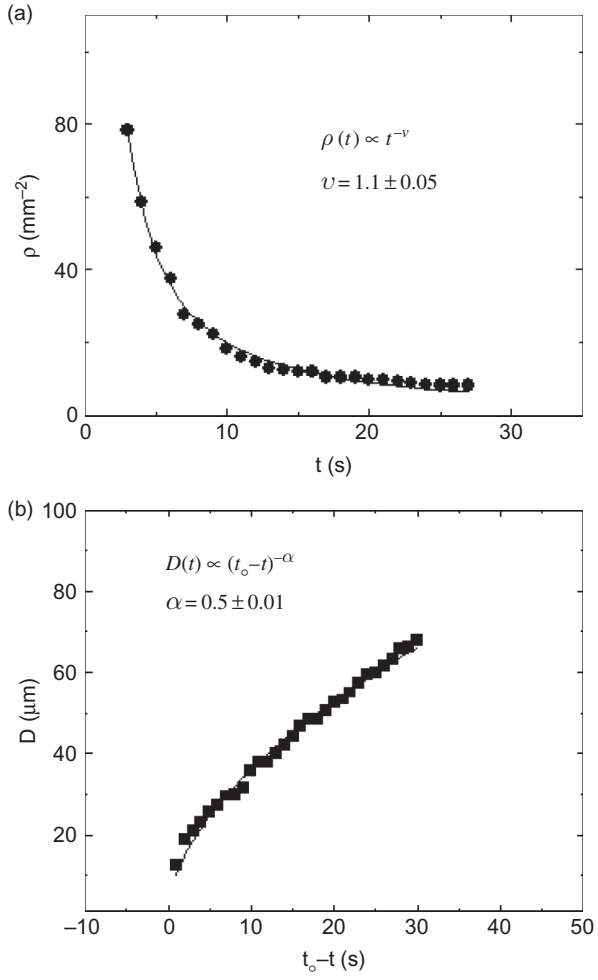

Figure 11. (a) Time evolution of defect density $\rho(t)$. The continuous line is the best fit to the theoretical Equation (1) with the exponent $\upsilon = 1.1 \pm 0.05$. (b) Time evolution of defect pair separation $D(t)$. The continuous line is the best fit to the theoretical Equation (2) with the exponent $\alpha = 0.55 \pm 0.01$.

the time dependences of the defect density and the inter-defect separation are consistent with the results of previous studies.

Acknowledgements

We thank Professor K.P.N. Murthy, School of Physics, University of Hyderabad for various useful discussions. SD and AK gratefully acknowledge the support from the UGC-CAS, School of Physics. We acknowledge Asahi Glass for supplying CYTOP.

References

[1] Dierking, I. *Textures of Liquid Crystals*; Wiley-VCH Verlag GmbH and Co. KGaA: Weinheim, 2003.
[2] de Gennes, P.G. *The Physics of Liquid Crystals*, 2nd ed.; Clarendon: Oxford, 1993.
[3] Chandrasekhar, S. *Liquid Crystals*; Cambridge University Press: Cambridge, 1977.
[4] Chaikin, P.M.; Lubensky, T.C. *Principle of Condensed Matter Physics*; Cambridge University Press: Cambridge, 1998.
[5] Frank, F.C. *Disc. Farady Soc*. **1958**, *25*, 19(1–10).
[6] Nehring, J.; Saupe, A. *J. Chem. Soc., Faraday Trans. II* **1972**, *68*, 1–15.
[7] Cladis, P.E.; Kleman, M. *J. Phys. (Paris)* **1972**, *33*, 591(1–8).
[8] Cladis, P.E.; Saarloos, W.V.; Finn, P.L.; Kartan, A.R. *Phys. Rev. Lett*. **1987**, *58*, 222(1–4).
[9] Meyer, R.B. *Phil. Mag*. **1973**, *27*, 405(1–21).
[10] Kleman, M. *Advances in Liquid Crystals*, Vol. 1: Brown, G.H., Ed.; Academic Press: New York, 1975.
[11] Pargellis, A.; Turok, N.; Yurke, B. *Phys, Rev. Lett*. **1991**, *67*, 1570(1–4).
[12] Nagaya, T.; Hotta, H.; Orihara, H.; Ishibashi, Y. *J. Phys. Soc. Jpn* **1991**, *60*, 1572(1–7).
[13] Nagaya, T.; Hotta, H.; Orihara, H.; Ishibashi, Y. *J. Phys. Soc. Jpn* **1992**, *61*, 3511(1–7).
[14] Minoura, K.; Kimura, Y.; Ito, K.; Hayakawa, R.; Miura, T. *Phys. Rev. E*: *Stat., Nonlinear, Soft Matter Phys*. **1998**, *58*, 643(1–7).
[15] Dafemous, C.M. *Quart. J. Mech. Appl. Math (UK)* **1970**, *23*, S49(1–16).
[16] Lavrentovich, O.D. *et al. Defects in Liquid Crystals: Computer Simulations, Theory and Experiments (NATO Science Series Mathematics, Physics and Chemistry*, Vol. 43); Kluwer Academic Publishers: Dordrecht, 2001.
[17] Bogi, A. *et al. Phys. Rev. Lett*. **2002**, *89*, 225501(1–4).
[18] Blanc, C. *et al. Phys. Rev. Lett*. **2005**, *95*, 097802(1–4).
[19] Oswald, P.; Mullol, J.I. *Phys. Rev. Lett*. **2005**, *95*, 027801(1–4).
[20] Dierking, I.; Marshall, O.; Wright, J.; Bullied, N. *Phys. Rev. E*: *Stat., Nonlinear, Soft Matter Phys*. **2005**, *71*, 061709(1–6).
[21] Dhara, S. *et al. Phys. Rev. E*: *Stat., Nonlinear, Soft Matter Phys*. **2009**, *79*, 060701(1–4).
[22] Arun Kumar, T.; Sathyanarayana, P.; Sastry, V.S.S.; Takezoe, H.; Madhusudana, N.V.; Dhara, S. *Phys. Rev. E*: *Stat., Nonlinear, Soft Matter Phys*. **2010**, *82*, 011701(1–6).
[23] Dhara, S.; Kumar, T.A.; Ishikawa, K.; Takezoe, H. *J. Phys. Condens. Matter* **2009**, *21*, 505103(1–5).
[24] Kim, J.K.; Araoka, F.; Jeong, S.M.; Dhara, S.; Ishikawa, K.; Takezoe, H. *Appl. Phys. Lett*. **2009**, *95*, 063505(1–3).
[25] Kim, J.K.; Le, K.V.; Dhara, S.; Araoka, F.; Ishikawa, K.; Takezoe, H. *J. Appl. Phys*. **2010**, *107*, 123108(1–4).
[26] Jeong, S.M.; Kim, J.K.; Shimbo, Y.; Araoka, F.; Dhara, S.; Ha, N.Y.; Ishikawa, K.; Takezoe, H. *Adv. Mater*. **2010**, *22*, 34(1–5).
[27] Dhara, S.; Madhusudana, N.V. *Europhys. Lett*. **2004**, *67*, 411(1–7).
[28] Dhara, S.; Madhusudana, N.V. *Euro. Phys. J. E* **2007**, *22*, 139(1–10).
[29] Dhara, S.; Le, K.V.; Takanishi, Y.; Takezoe, H. *Jpn J. Appl. Phys*. **2007**, *46*, 5920(1–4).
[30] Dhara, S.; Madhusudana, N.V. *Phase Transition* **2008**, *81*, 561(1–9).
[31] Kleman, M.; Lavrentovich, O.D. *Phil. Mag*. **2006**, *86*, 4117(1–20).